VOL. 3, NO. 5, OCTOBER 2008 ISSN 1819-6608
ARPN Journal of Engineering and Applied Sciences

www.arpnjournals.com

EXPERIMENTAL AND ANALYTICAL STUDY ON CHIP FORMATION MECHANISM IN MACHINING OF DRACs

Raviraj Shetty, Laxmikanth Keni, R. Pai and V. Kamath
Department of Mechanical and Manufacturing Engineering, Manipal Institute of Technology, Karnataka, India
E-Mail: rrshetty2@rediffmail.com

ABSTRACT

It is known from the theory of metal cutting that an examination of machining chips provides the cheapest and the most effective way of understanding the machining characteristics of a material. The review of literature on machining of DRACs reveals that these aspects have been given relatively little attention during the machining studies. This viewpoint has provided motivation for the study of fundamental aspects of machining of composites involving chip formation mechanism experimentally and analytically.

This paper discusses experimental work and finite element analysis to investigate the mechanism of chip formation during machining of DRACs. Focus of this paper is on understanding the influence of different cutting parameters on mechanism of machining. Chips generated experimentally and by finite element modeling during orthogonal machining of DRACs were used for this purpose.

Keywords: discontinuously reinforced aluminium composites, finite element method, chip formation mechanism.

Nomenclature

s_y = Yield stress.
s_o = initial yield stress
ε = Strain rate
C and P = Cowper-Symonds strain rate
e_{eff} = Effective plastic strain.
β = Hardening parameter.
E_P = Plastic hardening modulus.
E_{tan} = Tangent modulus.
E = Modulus of elasticity
τ_{lim} = limiting shear stress
τ = equivalent shear stress
P = contact pressure
μ = Friction of coefficient
b = Cohesion sliding resistance

1. INTRODUCTION

The DRACs are considered to be one of the 'difficult to machine' materials. Discontinuously reinforced aluminium composites (DRACs) derive their excellent mechanical properties from the combination of a hard reinforcement phase such as silicon carbide (SiC) and a ductile matrix material such as aluminum or magnesium. While current applications for this class of materials are primarily limited to aerospace and automotive applications, their development continues with resulting new products such as high voltage power transmission lines and heat sinks for electronic components [Evans et al., 2003]. Machining of DRACs can be attempted by conventional and non conventional machining methods. During the conventional machining of DRACs, various factors like cutting tool wear rate, cutting forces, surface quality have been used as a criteria to assess their machinability [Brun and Lee, 1985; Chadwick and Heath, 1990; Tomac and Tonnensen, 1992; Looney *et al.*, 1992; Monaghan and O'Reilly, 1992a, 1992b; Weinert, 1993; Shetty *et al.* 2007,2008]. The fundamental aspects of machining such as chip formation during their machining have hardly been dealt with anywhere except by [Monaghan, 1994; Shetty *et al.* 2007]. Non conventional machining of composites is discussed in [Felloni *et al.*, 1994; Lau *et al.*, 1995; Yue and Dai, 1996]. Hence, it is necessary to understand the chip formation mechanism for this material through further investigation. This will render the material more suitable for advanced applications and more efficient chip control in machining can also be achieved.

The aim of the paper is to present the mechanisms of the chip formation, while machining DRACs. Experimental and analytical investigations were carried out in orthogonal cutting conditions. The mechanism of the chip formation was studied for various values of cutting parameters.

2. EXPERIMENTAL METHOD

Al-SiC MMC workpiece specimens popularly known as DRACs having aluminum alloy 6061 as the matrix and containing 15 vol. % of silicon carbide particles of mean diameter 25µm in the form of cylindrical bars of length 120mm and diameter 40 mm manufactured in Vikram Sarbhai Space Centre (VSSC) Trivandrum by Stir casting process with pouring temperature 700-710°C, stirring rate 195 rpm, extrusion at 457°C, extrusion ratio 30:1, direct extrusion speed 6.1 m/min to produce Ø40mm cylindrical bars. The specimens were solution treated for 2h at a temperature of 540°C in a muffle furnace, Temperatures were accurate to within ±2 °C and quench delays in all cases were within 20 s. after solutionising, the samples were water quenched to room temperature, and subsequently aged for six different times to obtain samples with different Brinell hardness number (BHN), out of which one samples were selected, one with 94 BHN obtained at peakage condition i.e. 2h at 220°C respectively. Sample selected were kept in a refrigerator right after the heat treatments. Figure-1 shows the SEM

image of DRACs containing 6061 Al and 15vol. % SiC particles of 25μm. The chemical composition of specimens is shown in Table-1. Turning method as machining process was selected. The experimental study was carried out in PSG A141 lathe (2.2 KW) with different cutting speed (45,73,101 m/min) and constant rake angle (0^o), feed (0.11 mm/rev), depth of cut (0.25mm). The selected cutting tool was cubic boron nitride inserts KB-90 (ISO code), for machining of MMC materials. Surface condition of chips formed was observed using JEOL JSM-6380LA Analytical Scanning Electron Microscope.

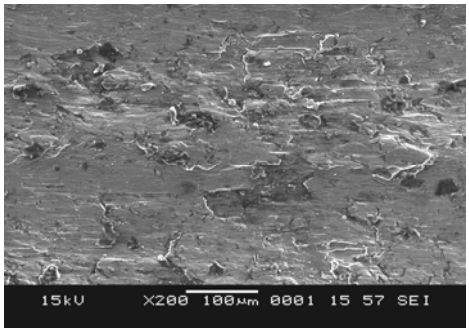

Figure-1. SEM image of DRACs (6061 Al/ 15% SiC 25p)

Table-1. Nominal chemical composition of Base metal (6061 Al alloy).

Elements	Cu	Mg	Si	Cr	Al
Weight (%)	0.25	1.0	0.6	0.25	Balance

3. FINITE ELEMENT METHOD

3.1 Material modeling

The DRACs work material was a 6061 aluminum alloy reinforced with silicon carbide particles. A temperature-independent plastic kinematics material model (from ANSYS/LS-DYNA) and associative flow rule were used for the matrix. Strain rate was accounted for using the Cowper-Symonds model which scaled the yield stress by a strain rate dependent factor. According to ANSYS/LSDYNA manual the equation to calculate yield stress in the plastic kinematics material model is given below:

$$\sigma y = \left[1 + \left(\frac{\dot{\varepsilon}}{C}\right)^{1/p}\right]\left(\sigma + \beta E_P \varepsilon_p^{eff}\right)$$

Where

$$E_P = \left(\frac{E_{\tan} E}{E - E_{\tan}}\right)$$

Here σ_y, is the yield stress, σ_0, the initial yield stress, $\dot{\varepsilon}$ the strain rate, C and P are the Cowper-Symonds strain rate parameters, ε_{eff} the effective plastic strain, β, the hardening parameter (0 for kinematic hardening and 1 for isotropic hardening from ANSYS/LSDYNA manual) and E_p, the plastic hardening modulus, E_{tan}, the tangent modulus, E, the modulus of elasticity. The material properties of the matrix were based on the commonly accepted values σ0 = 125 MPa, E = 71 GPa, Etan = 1.48 GPa from [Meijer et al., 2000 and Long et al., 2005]. Values of Cowper-Symonds strain rate parameters (C = 6500, P = 4) for aluminum alloy were taken form ANSYS/LSDYNA manual. In this study kinematic hardening was considered as a first assumption because of comparatively low plastic hardening modulus (1.51 GPa) of matrix material and to investigate the strain rate effect.

A Strain based chip separation criterion available with ANSYS/LSDYNA for this material model was used in the simulation. According to this criterion, chip separation occurs when the strain value of the leading node is greater than or equal to a limiting value. Based on the work for aluminum alloys reported in [Zhang *et al.*, 1995], the limiting strain was taken as 1. When an element of matrix material reached the limiting strain value, the corresponding element would be deleted. Additionally, SiC particles were treated as an isotropic perfectly elastic material following the generalized Hook's law. For simplicity, particle fracture was not considered in the present model and debonding of particles was assumed to be due to failure of the matrix material around the particles. The material properties of the particles were based on the commonly accepted values: modulus of elasticity = 400 GPa and Poisson's ratio = 0.17.

3.2 Boundary conditions

A two-dimensional finite element model was constructed using explicit finite element software package ANSYS/LSDYNA, version 11. Lagrangian formulation was used for material continuum to develop the plane-stress model. The geometry of machining is shown in Fig. 2. In accordance with practice, the tool cutting edge was assumed to have a 0.02mm nose radius. The reinforcement particles were introduced around the cutting line and restricted to a small area to keep the model size manageable. In order to facilitate the study of particle interaction at different locations of the tool rake face, rows of reinforcements were perpendicular to the cutting direction. The particles (25μm diameter) were 15% by volume in this region and were assumed to be perfectly bonded with the matrix. Similar to the work reported in [Monaghan and Brazil, 1997], the interface nodes of the matrix and reinforcements were tied together; therefore the initial displacements at the interface are equal for both the matrix and reinforcements. Since the interface is very hard and brittle and hence similar to the particles [Zhu et al., 2005], the interface was considered as an extension of the particle. The cutting tool was treated as a rigid body and moved horizontally into the workpiece at three different speeds i.e. 45m/min, 73m/min and 101m/min with depth of cut 0.5mm and 0^0 rake angle. The workpiece was fully fixed on its bottom surface to eliminate rigid body motion.

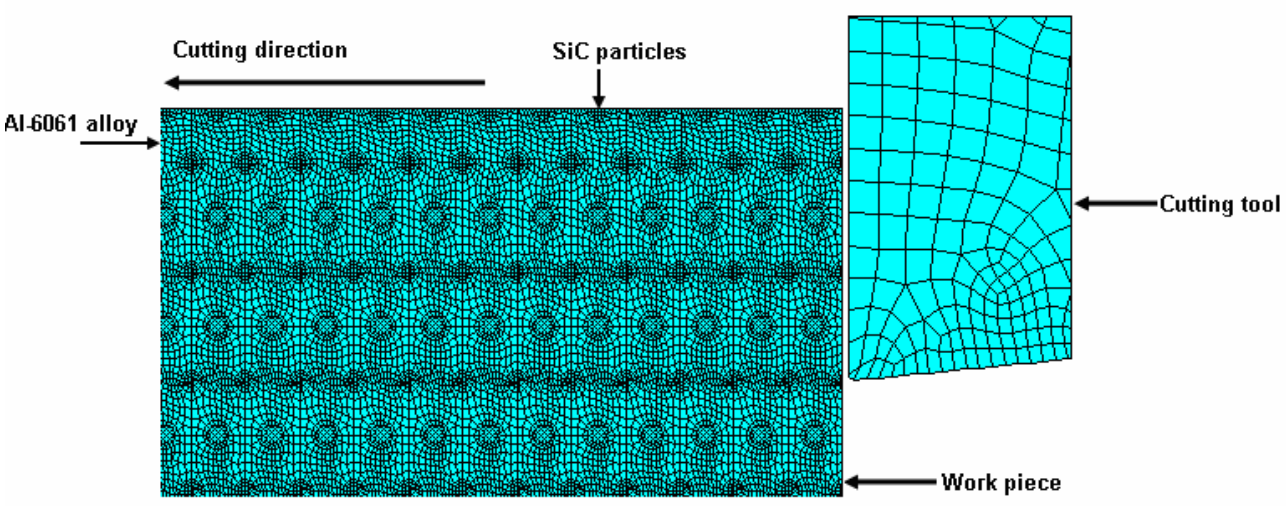

Figure-2. Finite element mesh for DRACs.

3.3 Contact and friction

Along with the general contact family in ANSYS/LSDYNA, the automatic contact options are the most commonly used contact algorithms for its versatility. Hence, 2D automatic contact was chosen for this simulation. In order to consider the effect of friction along the tool–chip interface, Coulomb friction model was employed. This is defined as

$$\tau_{\lim} = \mu P + b$$

$$|\tau| \le \tau_{\lim}$$

Where τ_{lim}, is the limiting shear stress, τ, the equivalent shear stress, P, the contact pressure, μ, the friction coefficient and b, the cohesion sliding resistance (sliding resistance with zero normal pressure). According to ANSYS/LS-DYNA manual, two contacting surfaces can carry shear stresses up to a certain magnitude across their interface before they start sliding relative to each other (sticking state). When $\tau > \tau lim$, the two surfaces will slide relative to each other (sliding state). For machining conditions b was assumed to be zero. The limiting shear stress τlim = 202 MPa and coefficient of friction, μ = 0.62 were based on the study reported in [Pramanik et al., 2006].

4. RESULTS AND DISCUSSIONS

The form of chip produced is one of the major parameters influencing productivity in metal cutting industry. Generally, there are two groups of chip forms, (1) acceptable chips and (2) unacceptable chips, for convenience of handling. Acceptable chips do not interfere with the work or machine tool and cause no problems of disposal. Unacceptable chips interrupt regular manufacturing operation, as they tend to entangle the tool and work piece and safety problems to operators. Entangling chips can harm the surface finish and even lead to unexpected tool failure.

4.1 Chip formation mechanism (experimental)

Typical chips were formed from most experimental runs during the machining (turning) of 6061Aluminium 15Vol. % SiC(p) composites in dry cutting under different cutting conditions as shown in Figure-3. The chips produced were either continuous saw toothed or semi continuous saw toothed depending upon the cutting conditions.

An enlarged cross-section of a chip shows a prominently formed saw tooth profile on the outer surface of the chip Figure-4. The remaining portion of the chip appears plain without any major cracks. This indicates that during the deformation, a gross fracture initiates on the chip free surface and propagates towards the tool nose across the thickness of the chip. The gross fracture is usually terminated half-way, and the remaining portion of the chip is removed by flow-type deformation. The actual pattern of the development of deformation can be seen from the SEM photograph of chip root Figure-5.

The influence of cutting speed is equivalent to the effect of strain rate and temperature on the deformation. At low cutting speed, the strain rate is low and low temperature deformation occurs. Whereas, at higher cutting speeds the strain rate is high and temperature deformation occurs. Therefore during machining at lower cuttings speeds, material behaves in a brittle manner with little influence of either temperature or strain rate. Moreover at lower cutting speeds, the displacement of reinforcement particles is less, which generates voids by either displacement or fragmentation of reinforcement particles. Hence, brittle failure becomes more prominent. This causes the formation of saw tooth profile on the chip. The effect becomes more pronounced if the cutting speed increases.

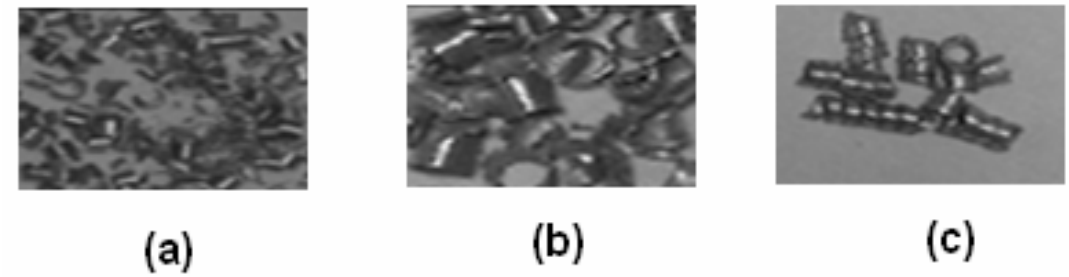

Figure-3. Saw toothed chips formed from experimental runs under different cutting condition 45m/min (b) 73m/min (c) 101m/min

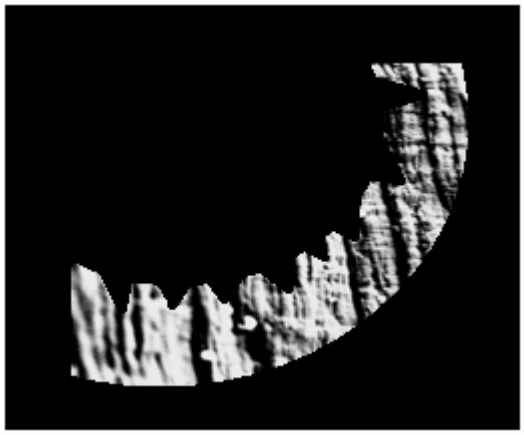

Figure-4. SEM image of longitudinal cross-section of saw toothed chip.

Figure-5. SEM image of saw toothed chip root.

4.2 Chip formation mechanism (finite element modeling)

ANSYS/LS-DYNA supplies several formulations for numerical modelling: Lagrangian, Eulerian and Arbitrary Lagrangian Eulerian (ALE). Among them, Lagrangian and ALE formulations supply approaches to chip separation in the chip formation process.

Lagrangian formulation tracks discrete material points. Chip separation is normally performed along predetermined lines of elements on the moving path of the tool edge, by deleting elements ahead the tool edge when element failure criterion, such as strain failure criterion, is reached. In addition, the number and size of deleted elements affect produced chip thickness, and fine elements improve simulated result whereas at the same time increase sharply the calculation time and cost. Therefore, sharp tool is most frequently used in chip formation modeling, because the separation line is obvious and by using very fine elements along this line and defining strain failure only to these line elements.

In normal turning operation, cutting depth, feed rate and cutting speed are kept constant, and steady state will be reached within several seconds after the entrance of tool edge into work material. Knowledge about the shape and geometry of the formed chip is the prerequisite of steady-state modelling, which comes from experiment or simulation. This paper supplies a complete modelling method of initial chip formation. The work has a size of 6mm x 2mm, Moreover, in this analysis, the cutting tool is considered as rigid body, whereas workpiece has to be modelled as a deformable body in order to obtain the necessary chip formation mechanism. At the beginning, the tool is at the right side of the work, and as the tool advances, according to the surface crack mechanism a crack initiates on the free surface, extends to the cutting edge, and stops somewhere within the chip due to excessive compression. If a small crack occurs, it will trigger adiabatic shearing, but it is found that shear localization could also occur without a pre existing crack. Therefore, the determination of whether a crack exists will help clarify the chip formation mechanism. This leads to the Saw-tooth chip formation.

Figure-6 shows the form of the chips during the machining of DRACs at various cutting speeds. At lower cutting speed, the free surface of the chips of DRACs shows very little waviness. As the cutting speed increases the outer surface of the chips show formation of prominent saw tooth profile. Further higher cutting speeds result in higher cutting temperatures and consequently, an increase in the ductility of the material. So, with high cutting speed, saw toothed chip sizes may get longer without breaking.

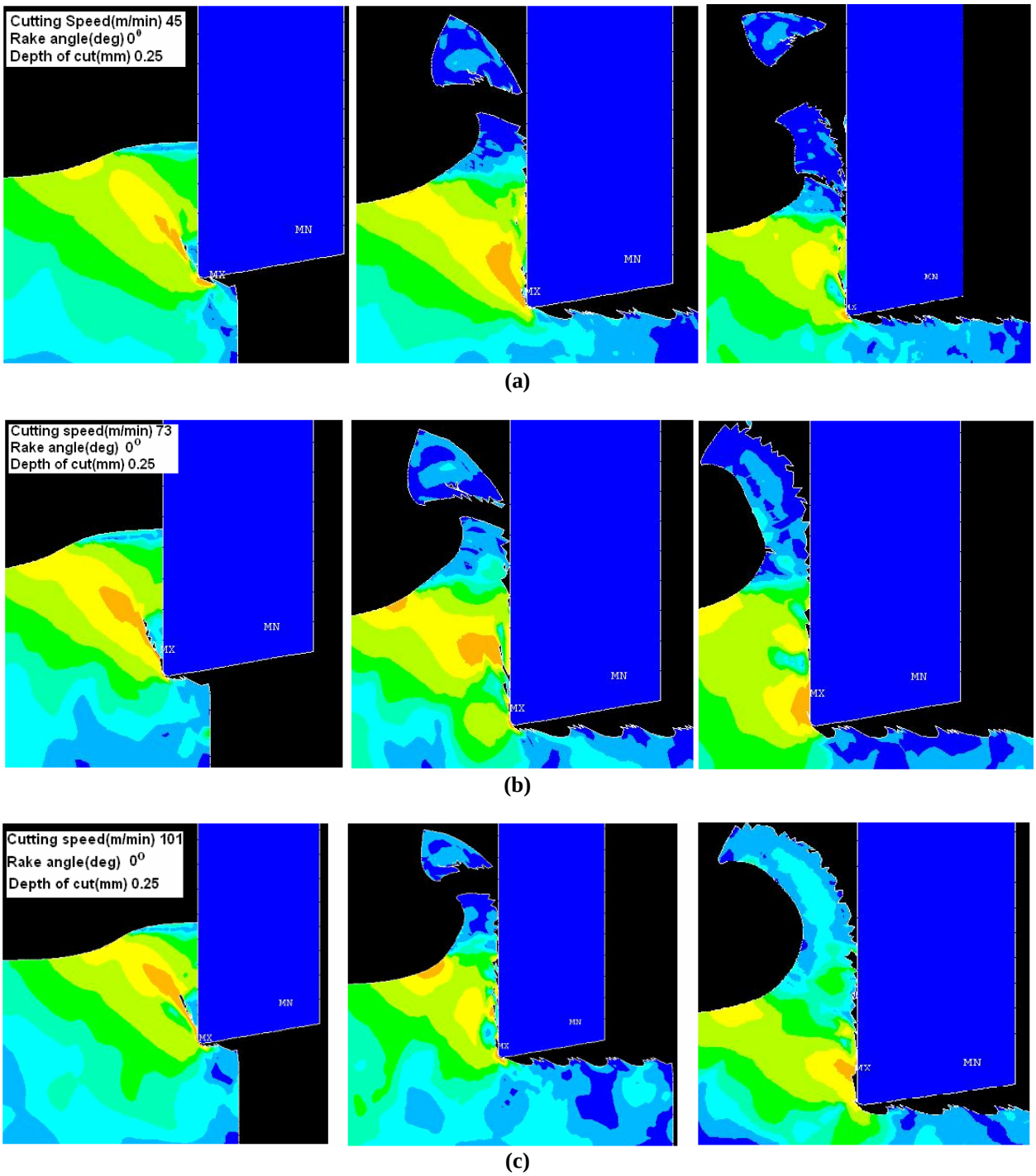

Figure-6. Progression of saw toothed discontinuous chips under different cutting condition (a) 45m/min (b) 73 m/min (c) 101m/min

5. CONCLUSIONS

Following conclusions can be drawn based on physical characteristics of the chips, micro structural study of chip formation, finite element modeling of chip formation mechanism during machining of DRACs.

- Chips of DRACs were found to curl through circles of wider and larger diameter as the cutting speed increases this may be due to sticking of work piece material on the tool face. The initial radius decreases with decrease in cutting speed. This could be due to changes in the length of contact on to tool face.
- The chip formation mechanism, during the machining of DRACs is mainly influenced by cutting speed. Increase in cutting speed results in the decrease in saw toothed chip.

- At higher cutting speed, the mechanism of deformation on shear plane involves local weakening of material due to intense heat generation.
- The mechanism of chip formation in DRACs involves the initiation of gross fracture at the free surface of the chip.
- The simulated chip morphology generally correlated well with the experimental data.

REFERENCES

ANSYS/LS-DYNA. Reference Manual Release 10. Livermore Software Technology Corporation, Livermore, CA. www.lstc.com.

Brun M.K and Lee M. 1985. Wear Characteristics of Various Hard Materials for Machining of SiC-reinforced Aluminium Alloy. Wear. Vol. 104, pp. 21-29.

Chadwick G.A and Health P.J. 1990. Machining of Metal Matrix Composites. Metals and Materials. pp. 73-76.

Evans A Marchi C.S Mortenson. 2003. A Journal of Metal Matrix Composites in Industry an Introduction and a Survey Kluwer Boston.

Felloni L Gatto Ippolito A. and Iuliano R. 1994. WED machinability of a 25% SiCp Reinforced 6061/Al alloy composite. PD-Vol. 64-2, Engineering Systems Design and Analysis, Vol. 2, ASME. pp. 70-85.

Lau W.S, Yue T.M., Lee T.C. and Lee W.B. 1995. Unconventional machining of composite Materials. J. Mater. Proc. Technol. 48: 199-205.

Long S.G., Zhou Y.C. 2005. Thermal fatigue of particle reinforced metal–matrix composite induced by laser heating and mechanical load. Composites Science and Technology. Vol. 65, pp. 1391-1400.

Looney L A Monaghan J M. O Reilly P and Taplin D M. R. 1992. The turning of an Al/SiC metal-matrix composite. J. of Mat. Proc. Technol. 33(4): 453-468.

Meijer G. Ellyin F. Xia Z. 2000. Aspects of residual thermal stress/strain in particle reinforced metal matrix composites. Composites: Part-B. Vol. 31, pp.29-37.

Monaghan J. Brazil D. 1997. Modeling the flow processes of a particle reinforced metal matrix composite during machining. Composites. Vol. 29A, pp. 87-99.

Monaghan J.M. 1994. The Use of Quick Stop Test to Study the Chip Formation of a SiC/Al Metal Matrix Composite and its Matrix Alloy. J. of Proc. of Adv. Mat. Vol. 4, pp. 170-179.

Monaghan J.M. and O'Reilly. 1992. Machinability of an Aluminium Alloy/Silicon Carbide Metal Matrix Composites. Processing of Advanced Materials. Vol. 9. pp. 37-46.

Monaghan J.M. and O'Reilly. 1992. The drilling of an al/SiC Metal Matrix Composite. J. Mater. Proc. Techno. Vol. 33, pp. 469-480.

Pramanik A., Zhang L.C., Arsecularatne J.A. 2006. Prediction of cutting forces in machining of metal matrix composites. International Journal of Machine Tools and Manufacturing. Vol. 46, pp.1795-1803.

Shetty Raviraj Pai, R.B. Rao S.S. Kamath V. 2008. Machinability study on discontinuously reinforced aluminium composites DRACs using response surface methodology and Taguchi's design of experiments under dry cutting condition. Maejo International Journal of Science and Technology. 2(01): 227-239.

Shetty Raviraj Pai R.B. Rao S.S., Kumar D. 2007. Chip and built-up edge formation in turning age hardened AA6061/15 vol. % SiCp composites with steam as coolant. In: Proceedings of 2nd International conference on recent advances in composite materials, ICRAM, New Delhi, India.

Tomac N. and Tonnensen K. 1992. Machinability of Particulate Aluminium Matrix Composites. Annals of CIRP. 31(1): 81-84.

Weinert K. 1993. Considerations of tool wear mechanism when machining MMCs. Ann. CIRP. Vol. 42, pp. 95-98.

Yue T.M. and Dai Y. 1996. Wire electric discharge machining of Al_2O_3 Particle and Short Fibre reinforced Aluminium based composites. Mater. Sci. Technol. Vol. 12, pp. 831-835.

Zhang Z.F., Zhang L.C., Mai Y.W. 1995. Particle effects on friction and wear of aluminium matrix composites. Journal of Materials Science. 30(23): 5999-6004.

Zhu Y. Kishawy H.A. 2005. Influence of alumina particles on the mechanics of machining metal matrix composites. International Journal of Machine Tools and Manufacturing. Vol. 45, pp. 389-398.